Bioorganic & Medicinal Chemistry Letters 24 (2014) 1923–1927

Contents lists available at ScienceDirect

Bioorganic & Medicinal Chemistry Letters

journal homepage: www.elsevier.com/locate/bmcl

Highly potent and selective 3-*N*-methylquinazoline-4(*3H*)-one based inhibitors of B-Raf^{V600E} kinase

Steve Wenglowsky [a], Li Ren [a,*], Jonas Grina [a], Joshua D. Hansen [a], Ellen R. Laird [a], David Moreno [a], Victoria Dinkel [a], Susan L. Gloor [a], Gregg Hastings [a], Sumeet Rana [a], Kevin Rasor [a], Hillary L. Sturgis [a], Walter C. Voegtli [a], Guy Vigers [a], Brandon Willis [a], Simon Mathieu [b], Joachim Rudolph [b]

[a] *Array BioPharma, Inc., 3200 Walnut Street, Boulder, CO 80301, United States*
[b] *Genentech, Inc., 1 DNA Way, South San Francisco, CA 94080-4990, United States*

ARTICLE INFO

Article history:
Received 10 February 2014
Revised 28 February 2014
Accepted 3 March 2014
Available online 13 March 2014

Keywords:
B-Raf inhibitors
Type IIB inhibitor
Kinase drug discovery
Melonoma

ABSTRACT

Herein we describe the design of a novel series of ATP competitive B-Raf inhibitors via structure-based methods. These 3-*N*-methylquinazoline-4(*3H*)-one based inhibitors exhibit both excellent cellular potency and striking B-Raf selectivity. Optimization led to the identification of compound **16**, a potent, selective and orally available agent with excellent pharmacokinetic properties and robust tumor growth inhibition in xenograft studies. Our work also demonstrates that by replacing an aryl amide with an aryl sulfonamide, a multikinase inhibitor such as AZ-628, can be converted to a selective B-Raf inhibitor, a finding that should have broad application in kinase drug discovery.

The Ras/Raf/MEK/ERK (MAPK) signaling pathway transduces signals from cell surface receptors to the nucleus leading to cellular proliferation, differentiation and survival.[1] Raf kinases act downstream of RAS and are responsible for MEK and ERK activation. BRAF gene mutations may lead to MAPK pathway amplification via constitutive activation of B-Raf. Mutated B-Raf is present in approximately 7% of all cancers,[2] and is most frequently associated with melanoma.[3,4] The most common (>90%) mutation in B-Raf is a glutamic acid for valine substitution at residue 600 (V600E),[2] which leads to constitutive kinase activity 500-fold greater than wild-type B-Raf,[5] and correlates with increased malignancy and decreased response to chemotherapy.[6] A number of drug candidates targeting the B-Raf^{V600E} mutation have been described, and recently two novel and selective B-Raf inhibitors vemurafenib[7] and dabrafenib[8] have shown impressive clinical results in the treatment of metastatic melonoma, thus validating B-Raf^{V600E} as a cancer target.

Our lab recently reported the discovery of several novel series of potent and selective inhibitors of B-Raf^{V600E},[9] that featured an amide linker connecting various hinge-binding templates to an aryl sulfonamide (Fig. 1). The aryl sulfonamide has been shown to be a key feature for engaging B-Raf in a DFG-in/αC-helix-out conformation, which confers significant enhancements in potency and selectivity. Although the amide linker functioned efficiently as a spacer and a conformational control, cleavage of the amide bond leading to the formation of potentially toxic aniline metabolites was observed in vivo for compound **1**. To address this potential liability, we initiated a program to identify alternative linkers.[10] Another approach was to rigidify and constrain the amide linker, exemplified by our recently disclosed discovery of a series of potent and selective inhibitors of B-Raf^{V600E} derived from the pyridopyrimidin-7-one template (compound **2**).[11] In parallel to this effort, we embarked on de novo design to identify new scaffolds. Our strategy was to retain the aryl sulfonamide moiety, and evaluate linker/hinge-binder combinations that could make a critical contact to the main chain-NH of Cys532 (Fig. 1).

Molecular modeling studies suggested that a quinoline nitrogen would be able to make the targeted hydrogen bond interaction when connected to the aryl sulfonamide via an amine linker at the 6-position (Fig. 2). Compound **3** was prepared to validate our hypothesis and showed sub-micromolar activity in the enzyme assay (Table 1).[12] Both the enzyme and cellular activity can be improved dramatically (>10×) when the quinoline hinge binding template was replaced by quinazoline **4**, an observation consistent with findings in the pyridopyrimidin-7-one series.[11] Potency was further enhanced by substituting the 2-fluoro substituent on the aryl sulfonamide with a chlorine. Compound **5** is now a single digit nanomolar inhibitor of B-Raf^{V600E} with a corresponding cellular IC_{50} of 44 nM.

* Corresponding author. Tel.: +1 303 386 1448; fax: +1 303 386 1130.
E-mail address: li.ren@arraybiopharma.com (L. Ren).

http://dx.doi.org/10.1016/j.bmcl.2014.03.007
0960-894X/

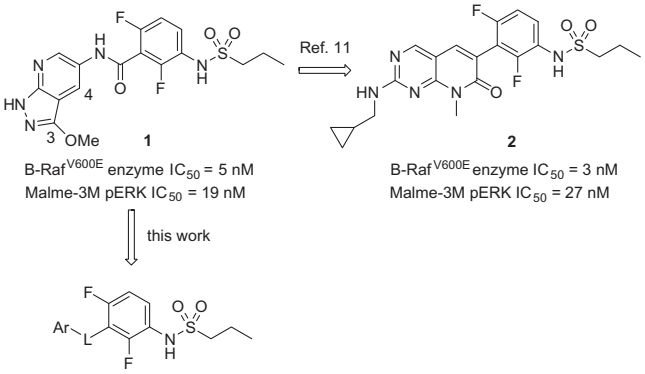

Figure 1. Schematic illustration of the amide linker replacement strategy.

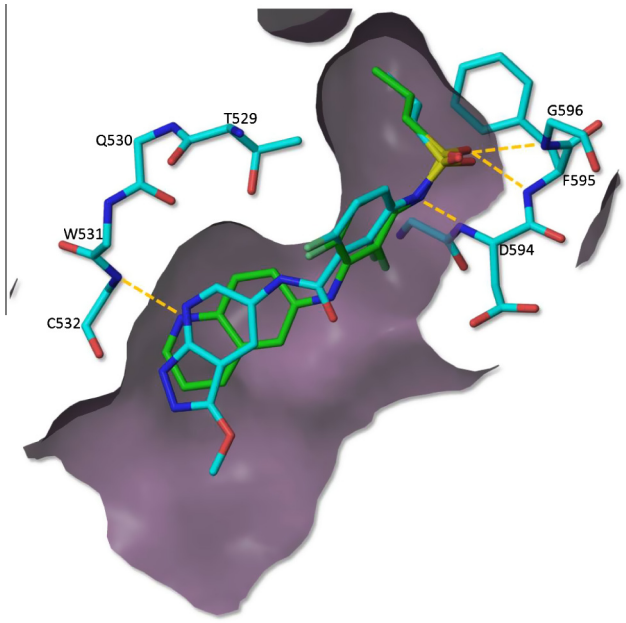

Figure 2. Model of **3** (green) compared with the X-ray crystal structure of **1** (blue) in complex with B-Raf^{WT}. The cleft surface is rendered in violet, and hydrogen-bonding interactions are shown as dashed yellow lines. Sidechains of the hinge residues are undisplayed for clarity. The propyl group resides in a pocket that is enlarged by an outward shift of the αC-helix. The DFG sequence (D594-G596) resides in its active (DFG-in) conformation. The model was generated by inspection and analogy to the X-ray crystal structure of **1** using the Maestro suite: Schrodinger Release 2009-1, Schrodinger LLC, New York, NY, 2009.

Keeping the 2-Cl substituent on the aryl sulfonamide constant and moving the nitrogen to the 4-position gave compound **6**, a quinoxaline analog with reduced activity. Further modifying the quinazoline template by substituting the 4-position with OMe, NHMe and NMe_2 (**7**–**9**) all led to potency loss, likely arising from steric interference with the P-loop. However, 3-*N*-methylquinazoline-4(3*H*)-one **10,** a regio-isomer of **7** (N- vs O-methylation), showed a 2× improvement in both biochemical and cellular potency over **5**. It is worth mentioning that AZ-628 (Fig. 3), a Type II multikinase inhibitor with B-Raf activity contains the same hinge binding motif.[13] We anticipated, however, that the aryl sufonamide tail would allow compound **10** to bind B-Raf in a type IIB fashion (i.e.; the DFG-in/αC-helix-out kinase conformation)[14], typically imparting excellent kinase selectivity (vide infra).

Comparing a model of **10** to the X-ray crystal structure of **1** suggests that the *N*-methyl group of **10** contacts residues at the exit of the ATP cleft, an area that was explored to balance potency

Table 1
B-Raf activity of compounds **3**–**12**

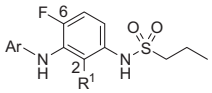

Compd	Ar	R^1	B-Raf^{V600E} IC_{50}[a] nM	pERK IC_{50}[a] nM
3	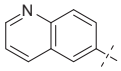	F	314	6251
4	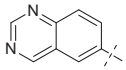	F	33	118
5	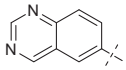	Cl	4	44
6	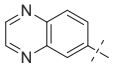	Cl	25	814
7	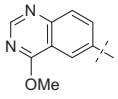	Cl	16	733
8	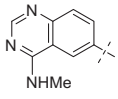	Cl	11	132
9	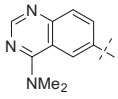	Cl	100	878
10	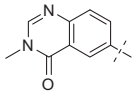	Cl	2	26
11	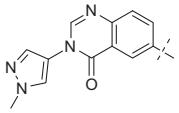	Cl	2	18
12	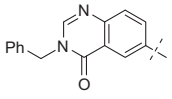	Cl	17	581

[a] IC_{50} values reflect the average from at least two separate experiments.

and physiochemical properties in the pyrazolo[1,5-*a*]pyrimidine[9e] and the imidazo[4,5-*b*]pyridine series.[9d] Indeed, the SAR trend mirrored our earlier findings. While a 5-membered heteroaryl such as methylpyrazole **11** was able to maintain co-planarity with the quinazoline-4(3*H*)-one hinge-binding template and make lipophilic contacts with several residues that form the exit from the ATP cleft[11] (i.e., Ile463, Trp531, Ser535, Ser536) and remained active, bulkier alkyl groups such as benzyl **12** resulted in significant potency loss owing to an out-of-plane steric clash with the outer edge of the cleft.

Having established the 3-*N*-methylquinazoline-4(3*H*)-one as a promising scaffold, the next stage of our optimization focused on varying the substitutions at the 2 and 6-position on the central phenyl ring. Selected examples are shown in Table 2. Among the halogens evaluated, the 2-Cl, 6-F substitution pattern gave the highest potencies both in biochemical and cellular assays (**10** vs **13** and **14**, **5** vs **4**). The potency of **14** can be rescued by replacing the 2-F with a CN group and compound **15** is a sub-nanomolar inhibitor of B-Raf^{V600E} with a pERK IC_{50} of 16 nM. Removing the 6-Cl substituent did not adversely affect activity as **16** remained similarly active, indicating that this position is less critical for potency than the 2-position. Indeed, compound **17**, an analog without

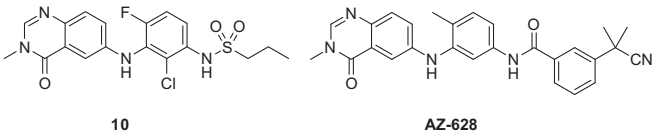

Figure 3. Structures of **10** and AZ-628.

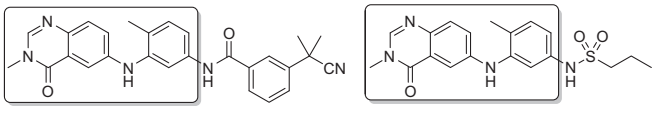

Figure 4. Structures of AZ-628 and **17**.

Table 2
B-Raf activity of compounds **10**, **13**–**17**

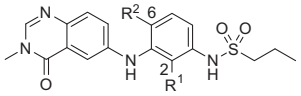

Compd	R^1, R^2	B-Raf^{V600E} IC_{50}[a] nM	pERK IC_{50}[a] nM
10	Cl, F	2	26
13	F, F	19	55
14	F, Cl	12	116
15	CN, Cl	0.2	16
16	CN, H	0.3	6
17	H, Me	851	—[b]

[a] IC_{50} values reflect the average from at least two separate experiments.
[b] Not determined.

Table 3
B-Raf activity of compounds **18**–**22**

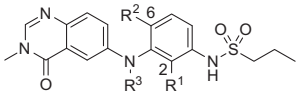

Compd	R^1, R^2	R^3	B-Raf^{V600E} IC_{50}[a] nM	pERK IC_{50}[a] nM
18	F, F	Me	11	62
19	F, Cl	Me	3	84
20	Cl, F	Me	8	114
21	F, F	Et	26	110
22	Cl, F	Et	30	603

[a] IC_{50} values reflect the average from at least two separate experiments.

Table 4
B-Raf activity of compounds **23**–**25**

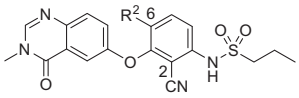

Compd	R^2	B-Raf^{V600E} IC_{50} nM[a]	pERK IC_{50} nM[a]
23	Cl	0.2	15
24	F	0.2	3
25	H	0.3	7

[a] IC_{50} values reflect the average from at least two separate experiments.

any substitution at the 2-position, showed very weak activity. These results are consistent with SAR from the amide[9b] and the pyridopyrimidin-7-one series[11] owing to the expectation that the aryl sufonamide occupies similar spaces. Possible explanations for the importance of the 2-position include: effects on torsion angle, hydrophobic contact with protein, and/or a beneficial effect on the pK_a of the sulfonamide motif.

Given the structural similarities between AZ-628 and **17** (same hinge binder, linker and phenyl spacer), the poor B-Raf^{V600E} activity of **17** was attributed to the different binding modes adopted by the sulfonamide versus the amide (Fig. 4).

The effect of modifying the linker was also investigated as modeling studies suggested the –NH linker was not making any specific interaction with the protein. It was reasoned that permeability and absorption could be improved by removing the unnecessary hydrogen bond donor. Alkylation of the linker nitrogen was examined and selected examples are shown in Table 3. For the 2-F analogs, methylation was well tolerated and no loss in activity was observed (**18** vs **13** and **19** vs **14**). The SAR was different for the 2-Cl series, where the –NMe linker led to a modest drop in potency (**20** vs **10**). The loss in potency likely arises from the larger Cl atom imparting an unfavorable dihedral angle between the two rings. Consistent with our hypothesis, larger alkyl group on the linker nitrogen also resulted in less active compounds (**21** vs **18** and **22** vs **20**).

The oxygen linker was also briefly evaluated and selected examples are shown in Table 4. Modeling evaluation predicted a slight shift of the template, suggesting that compounds should be similarly active. Synthetic accessibility led to the choice of the 2-CN series to test our hypothesis. IC_{50} values were comparable to the NH-linked counterparts (**23** vs **15**, **25** vs **16**), providing some of the most potent compounds within the series.

An X-ray crystal structure of B-Raf^{WT} in complex with **18** confirmed our anticipated binding mode and is depicted in Figure 5.[15] The quinazoline nitrogen makes a key H-bond to the NH of Cys532 at the hinge. The nitrogen atom of the sulfonamide moiety is within H-bond distance to the main-chain NH group of Asp594. Such an interaction suggests that the nitrogen atom is deprotonated, an observation consistant with previous reports from us[11] as well as others.[16] Meanwhile, an oxygen atom of the sulfonamide forms H-bonds to the backbone NH of Phe595 and G596 of the DFG sequence.

The *N*-linked 3-*N*-methylquinazoline-4(3*H*)-ones were prepared according to Scheme 1.[17] 6-Bromo-3-*N*-methylquinazoline-4(3*H*)-one **26** was used in a Buchwald coupling reaction with *N*-(3-amino-2-chloro-4-fluorophenyl)-1-cyclopropylmethanesulfonamide **27** to furnish compounds **10**–**22**.

The *O*-linked 3-*N*-methylquinazoline-4(3*H*)-ones were prepared according to Scheme 2.[17] 6-Hydroxyl-3-*N*-methylquinazoline-4(3*H*)-one **28** was coupled with 3-chloro-2,6-difluorobenzonitrile **29** in the presence of NaH to form the biaryl ether **30**. Displacing the 3-F with propyl sulfonamide under basic conditions gave compounds **23**–**25**.

General kinase selectivity for this series of compounds was expected to be excellent because of the uncommon DFG-in/αC-helix-out binding mode that is induced by the sulfonamide tail. Selected analogs such as **10** and **16** were screened in a large kinase panel at a concentration of 1 μM. For example, the inhibitory activity of **16** was assessed against a panel of 228 kinases[18] from across the human kinome at [ATP] ~ $K_{m,\ ATP}$. No kinase showed >60% inhibition other than B-Raf and C-Raf.

In vitro ADME properties of **10** and **16** were also determined (Table 5). Both compounds were highly permeable and intrinsically stable in mouse microsomes (Table 5). The in vivo profiles for both of them showed low clearance, high oral exposure and excellent bioavailability.

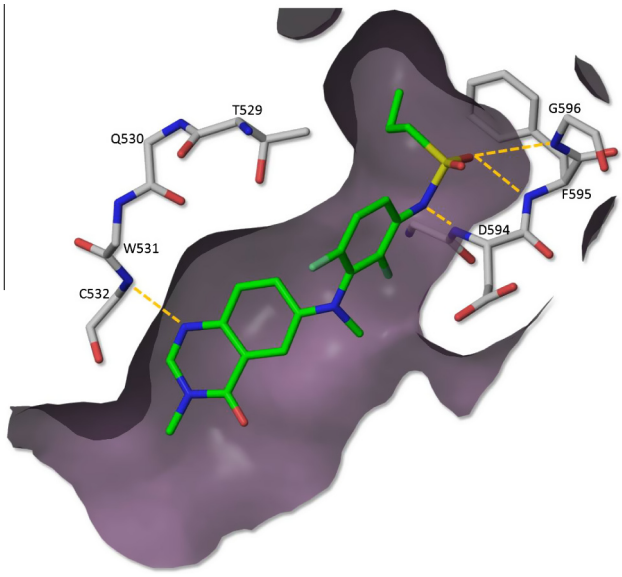

Figure 5. X-ray crystal structure of **18** in complex with B-Raf^{WT}. The protein is rendered white, and **18** is colored green. The surface and hydrogen-bonding interactions are as described in Figure 2, and the observed interactions are consistent with those depicted for compound **3**.

Compound **16** was further advanced to a tumor growth inhibition (TGI) study in nude mice with established LOX (B-Raf^{V600E}) xenografts, at a daily dose of 30 mg/kg QD from day 1 to day 4. Tumor volume was measured on day 1, 3, 5 and 8 (Fig. 6). After 4 days of dosing, a 95% TGI response was registered on day 5. More importantly, prolonged inhibition was observed even after dosing was stopped. For example, 99% TGI was reported on day 8. These findings suggest that compound **16** is a highly efficacious B-Raf inhibitor.

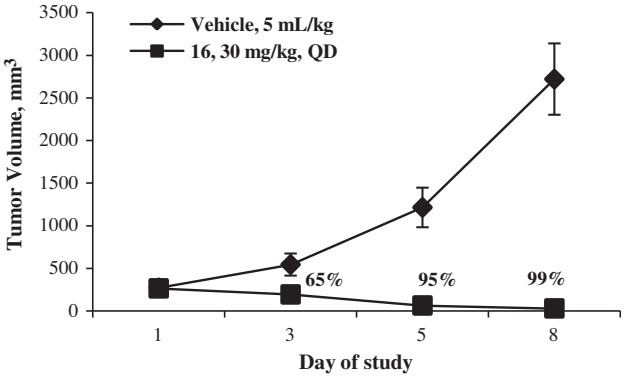

Figure 6. Tumor growth inhibition of **16** in LOX xenograft.

In summary, we have discovered a series of 3-*N*-methylquinazoline-4(*3H*)-one based B-Raf inhibitors with excellent potency and selectivity profiles, without the liability of releasing potentially toxic aniline metabolite associated with an earlier scaffold. Optimization led to the identification of compound **16**, a potent, selective and orally available B-Raf inhibitor with excellent pharmacokinetic properties and robust tumor growth inhibition in xenograft studies.

Additionally, our current work demonstrated that a type IIA multikinase inhibitor such as AZ-628 can be converted to a selective type IIB inhibitor by replacing an aryl amide with an aryl sulfonamide functionality (Fig. 7). Previously, we have also shown that the process can be reversed to rationally design a DFG-out multikinase inhibitor **31** from a DFG-in/αC-helix-out selective B-Raf inhibitor such as **1**.[19] Although these findings were discovered in the context of B-Raf, application to other kinase targets should be considered in the future.

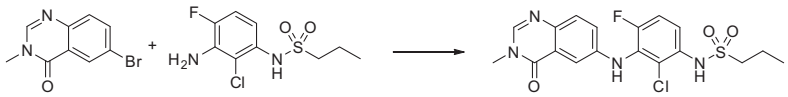

Scheme 1. Preparation of *N*-linked 3-*N*-methylquinazoline-4(3*H*)-ones. Reagents and conditions: $Pd_2(dba)_3$, BINAP, NaO*t*-Bu, PhMe, 100 °C.

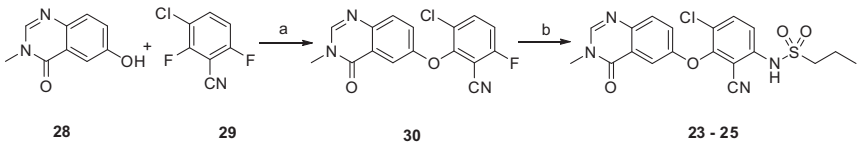

Scheme 2. Preparation of *O*-linked 3-*N*-methylquinazoline-4(*3H*)-ones. Reagents and conditions: (a) NaH, DMF; (b) *n*-PrSO_2NH_2, NaH, NMP, 40 °C, 30 min; then **30**, 120 °C, 4 h.

Table 5
In vitro ADME and pharmacokinetic properties of **10** & **16**

Compd	PappAB[a]	Microsome clearance[b]	Observed clearance[c]	Vd[d]	AUC[e]	%*F*
10	High	23	4.7	0.49	282	112
16	High	13	1.6	0.25	483	60

[a] LLC-PK1 cell permeability classification: low (<2 × 10^{-6} cm/s), medium (2–8 × 10^{-6} cm/s), high (>8 × 10^{-6} cm/s).
[b] Mouse microsome clearance (ml/min/kg).
[c] Mouse IV PK at 2.5 mg/kg (ml/min/kg).
[d] L/kg.
[e] Mouse PO PK at 30 mg/kg (μM h).

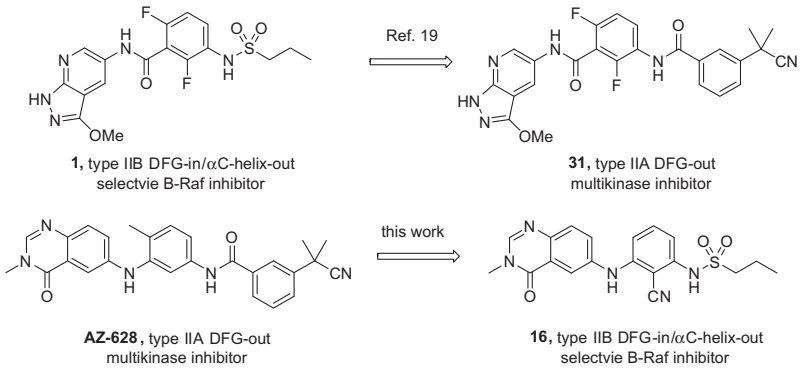

Figure 7. Conversion between type IIB selective B-Raf inhibitors and type IIA multikinase inhibitors.

Acknowledgment

The authors thank Susan Rhodes and Jennifer Otten for permeability determinations.

Supplementary data

Supplementary data associated with this article can be found, in the online version, at http://dx.doi.org/10.1016/j.bmcl.2014.03.007.

References and notes

1. Peyssonnaux, C.; Eychene, A. *Biol. Cell.* **2001**, *93*, 53.
2. Davies, H.; Bignell, G. R.; Cox, C.; Stephens, P.; Edkins, S.; Clegg, S.; Teague, J.; Woffendin, H.; Garnett, M. J.; Bottomley, W.; Davis, N.; Dicks, E.; Ewing, R.; Floyd, Y.; Gray, K.; Hall, S.; Hawes, R.; Hughes, J.; Kosmidou, V.; Menzies, A.; Mould, C.; Parker, A.; Stevens, C.; Watt, S.; Hooper, S.; Wilson, R.; Jayatilake, H.; Gusterson, B. A.; Cooper, C.; Shipley, J.; Hargrave, D.; Pritchard-Jones, K.; Maitland, N.; Chenevix-Trench, G.; Riggins, G. J.; Bigner, D. D.; Palmieri, G.; Cossu, A.; Flanagan, A.; Nicholson, A.; Ho, J. W. C.; Leung, S. Y.; Yuen, S. T.; Weber, B. L.; Seigler, H. F.; Darrow, T. L.; Paterson, H.; Marais, R.; Marshall, C. J.; Wooster, R.; Stratton, M. R.; Futreal, P. A. *Nature* **2002**, *417*, 949.
3. Pollock, P. M.; Harper, U. L.; Hansen, K. S.; Yudt, L. M.; Stark, M.; Robbins, C. M.; Moses, T. Y.; Hostetter, G.; Wagner, U.; Kakereka, J.; Salem, G.; Pohida, T.; Heenean, P.; Duray, P.; Kallioniemi, O.; Hayward, N. K.; Trent, J. M.; Meltzer, P. S. *Nat. Genet.* **2003**, *33*, 19.
4. (a) Gorden, A.; Osman, I.; Gai, W.; He, D.; Huang, W.; Davidson, A.; Houghton, A. N.; Busam, K.; Polsky, D. *Cancer Res.* **2003**, *63*, 3955; (b) Kuman, R.; Angelini, S.; Czene, K.; Sauroja, I.; Hahka-Kemppinen, M.; Pyrhonen, S.; Hemminki, K. *Clin. Cancer Res.* **2003**, *9*, 3362.
5. Wan, P. T.; Garnett, M. J.; Roe, S. M.; Lee, S.; Niculescu-Duvaz, D.; Good, V. M.; Jones, C. M.; Marshall, C. J.; Springer, C. J.; Barford, D.; Marais, R. *Cell* **2004**, *116*, 855.
6. (a) Samowitz, W. S.; Sweeney, C.; Herrick, J.; Albertsen, H.; Levin, T. R.; Murtaugh, M. A.; Wolff, R. K.; Slattery, M. L. *Cancer Res.* **2005**, *65*, 6063; (b) Riesco-Eizaguirre, G.; Gutiérrez-Martínez, P.; García-Cabezas, M. A.; Nistal, M.; Santisteban, P. *Endocr-Relat. Cancer* **2006**, *13*, 257; (c) Houben, R.; Becker, J. C.; Kappel, A.; Terheyden, P.; Bröcker, E. B.; Goetz, R.; Rapp, U. R. *J. Carcinog.* **2004**, *3*, 6.
7. Bollag, G.; Tsai, J.; Zhang, J.; Zhang, C.; Ibrahim, P.; Nolop, K.; Hirth, P. *Nat. Rev. Drug Disc.* **2012**, *11*, 873.
8. Rheault, T. R.; Stellwagen, J. C.; Adjabeng, G. M.; Hornberger, K. R.; Petro, K. G.; Waterson, A. G.; Dickerson, S. H.; Mook, R. A., Jr.; Laquerre, S. G.; King, A. J.; Rossanese, O. W.; Arnone, M. R.; Smitheman, K. N.; Kane-Carson, L. S.; Han, C.; Moorthy, G. S.; Moss, K. G.; Uehling, D. E. *ACS Med. Chem. Lett.* **2013**, *4*, 358.
9. (a) Wenglowsky, S.; Ren, L.; Ahrendt, K. A.; Laird, E. R.; Aliagas, I.; Alicke, B.; Buckmelter, A. J.; Choo, E. F.; Dinkel, V.; Feng, B.; Gloor, S. L.; Gould, S. E.; Gross, S.; Gunzner-Toste, J.; Hansen, J. D.; Hatzivassiliou, G.; Liu, B.; Malesky, K.; Mathieu, S.; Newhouse, B.; Raddatz, N. J.; Ran, Y.; Rana, S.; Randolph, N.; Risom, T.; Rudolph, J.; Savage, S.; Selby, L. T.; Shrag, M.; Song, K.; Sturgis, H. L.; Voegtli, W. C.; Wen, Z.; Willis, B. S.; Woessner, R. D.; Wu, W.-I.; Young, W. B.; Grina, J. *ACS Med. Chem. Lett.* **2011**, *2*, 342; (b) Wenglowsky, S.; Ahrendt, K. A.; Buckmelter, A. J.; Feng, B.; Gloor, S. L.; Gradl, S.; Grina, J.; Hansen, J. D.; Laird, E. R.; Lunghofer, P.; Mathieu, S.; Moreno, D.; Newhouse, B.; Ren, L.; Risom, T.; Rudolph, J.; Seo, J.; Sturgis, H. L.; Voegtli, W. C.; Wen, Z. *Bioorg. Med. Chem. Lett.* **2011**, *21*, 5533; (c) Wenglowsky, S.; Moreno, D.; Rudolph, J.; Ran, Y.; Ahrendt, K. A.; Arrigo, A.; Colsen, B.; Gloor, S. L.; Hasting, G. *Bioorg. Med. Chem. Lett.* **2012**, *22*, 912; (d) Newhouse, B. J.; Wenglowsky, S.; Grina, J.; Laird, E. R.; Voegtli, W. C.; Ren, L.; Ahrendt, K.; Buckmelter, A. J.; Gloor, S. L.; Klopfenstein, N.; Rudolph, J.; Wen, Z.; Li, X.; Feng, B. *Bioorg. Med. Chem. Lett.* **2013**, *23*, 5896; (e) Ren, L.; Laird, E.; Buckmelter, A. J.; Dinkel, V.; Gloor, S. L.; Grina, J.; Newhouse, B.; Rasor, K.; Hastings, G.; Gradl, S. N.; Rudolph, J. *Bioorg. Med. Chem. Lett.* **2012**, *22*, 1165.
10. Mathieu, S.; Gradl, S.; Ren, L.; Wen, Z.; Aliagas, I.; Gunzner-Toste, J.; Pulk, R.; Zhao, G.; Alicke, B.; Boggs, J.; Buckmelter, A.; Choo, E.; Dinkel, V.; Gloor, S.; Gould, S.; Hansen, J.; Hastings, G.; Hatzivassiliou, G.; Laird, E.; Moreno, D.; Ran, Y.; Voegtli, W.; Wenglowsky, S.; Grina, J.; Rudolph, J. *J. Med. Chem.* **2012**, *55*, 2869.
11. Ren, L.; Ahrendt, K. A.; Grina, J.; Laird, E.; Buckmelter, A. J.; Hansen, J. D.; Newhouse, B.; Moreno, D.; Wenglowsky, S.; Dinkel, V.; Gloor, S. L.; Hasting, G.; Rana, S.; Rasor, K.; Risom, T.; Sturgis, H. L.; Voegtli, W. C.; Mathieu, S. *Bioorg. Med. Chem. Lett.* **2012**, *22*, 3387.
12. Inhibitor enzyme activity was determined utilizing full-length B-Raf^{V600E}. Inhibition of basal ERK phosphorylation in Malme-3M cells was used as the mechanistic cellular assay. For assay description see: Laird, E.; Lyssikatos, J.; Welch, M.; Grina, J.; Hansen, J.; Newhouse, B.; Olivero, A.; Topolav, G. WO 2006/084015 A2, 2006.
13. Aquila, B.; Dakin, L.; Ezhuthachan, J.; Lee, S.; Lyne, P.; Ponntz, T.; Zheng, X. WO 2006/024834.
14. Wang, X.; Kim, J. *J. Med. Chem.* **2012**, *55*, 7332.
15. Coordinates for the B-raf crystal structure have been deposited in the PDB: accession code 4PP7.
16. Tsai, J.; Lee, J. T.; Wang, W.; Zhang, J.; Cho, H.; Mamo, S.; Bremer, R.; Gillette, S.; Kong, J.; Haass, N. K.; Sproesser, K.; Li, L.; Smalley, K. S. M.; Fong, D.; Zhu, Y.; Marimuthu, A.; Nguyen, H.; Lam, B.; Liu, J.; Cheung, I.; Rice, J.; Suzuki, Y.; Luu, C.; Settachatgul, C.; Shellooe, R.; Cantwell, J.; Kim, S.; Schlessinger, J.; Zhang, K. Y. J.; West, B. L.; Powell, B.; Habets, G.; Zhang, C.; Ibrahim, P. N.; Hirth, P.; Artis, D. R.; Herlyn, M.; Bollag, G. *Proc. Natl. Acad. Sci. U.S.A.* **2008**, *105*, 3041.
17. Grina, J.; Hansen, J.D.; Laird, E.R.; Mathieu, S.; Moreno, D.; Ren, L.; Rudolph, J.; Wenglowsky, S. M. WO 2012118492.
18. See Supporting information for the list of 228 kinases.
19. Wenglowsky, S.; Moreno, D.; Laird, E. R.; Gloor, S. L.; Ren, L.; Risom, T.; Rudolph, J.; Sturgis, H. L.; Voegtli, W. C. *Bioorg. Med. Chem. Lett.* **2012**, *22*, 6237.